Indian Journal of Pure & Applied Physics
Vol. 61, July 2023, pp. 535-540
DOI: 10.56042/ijpap.v61i7.105

Effect of Mirror Characteristics on Critical Coupling in Plasmonic Nanostructures

Jagathpriya L M & Shourya Dutta-Gupta*

Materials Science and Metallurgical Engineering, Indian Institute of Technology Hyderabad, Sangareddy 502 284, Telangana, India

Received 15 October 2022; accepted 12 June 2023

Plasmonic nanostructures have been used in various non-destructive sensing and modulation applications. The efficiency of plasmonic structures can be tuned by controlling their net optical absorption and near-field enhancement. In the current study, we numerically investigate the effect of mirror characteristics on absorption and near-field enhancement in critically coupled plasmonic structures. We explore structures with metallic mirrors and dielectric Bragg reflectors (DBR) and show that the optical response can be enhanced by a judicious choice of spacer thickness and operating wavelength. The results presented in this study provide a roadmap for designing plasmonic substrates with enhanced efficiencies.

Keywords: Plasmonics; Gold nanoparticles; Critical coupling; Perfect absorption

1 Introduction

Plasmonic nanostructures have been used to control and manipulate light well beyond the diffraction limit[1]. One of the major applications of plasmonic nanostructures is in the field of sensing[2–8]. Plasmonic sensors have been used for refractive index sensing, sensing bio-analytes and even for developing hydrogen gas sensors[2–8]. The superior performance of plasmonic sensors originates from the enhanced near-field in the vicinity of the plasmonic structures at resonance[1,9]. The resonance wavelength of the structure can be tuned by controlling the size, shape, arrangement, and materials used for the fabrication of the structures[10–18]. Wang *et al.* investigated the role of size and shape in refractive index sensing[10]. The refractive index sensitivity of the sensor could be increased by increasing the number of corners and by decreasing the radius of curvature. Furthermore, the resonance wavelength can be tuned by controlling the aspect ratio of the structures, with higher aspect-ratio structures exhibiting a red-shifted resonance. In addition to the plasmonic sensors based on single or few particles, it is possible to realize large-area plasmonic substrates with either periodic or non-periodic arrangement of individual plasmonic structures. Diffractive coupling in such periodic arrays can be used to generate plasmonic structures with high Q-factors[19]. The efficiency of the plasmonic structures can befurther enhanced by combining them with tailored substrates[20,21]. One approach towards this includes the exploitation of the phenomenon of critical coupling, namely, the efficient coupling of light into a plasmonic mode by controlling the various scattering channels[22,23]. Critical coupling can be achieved in layered structures by incorporating a mirror underneath the plasmonic structure. Thereby, the interference of light from the various interfaces can be used to tune the reflection and transmission. In such a structure, the dielectric spacer (between the plasmonic structure and the mirror) controls the phase difference between the two reflected waves from various interfaces. Under specific conditions, it is possible to ensure zero transmission and zero reflection; hence, all the light is absorbed by the structure, leading to perfect absorption[2,24–26]. Bulovic *et al.* demonstrated that an organic layer with sub-10 nm thickness can also be made to be perfectly absorbing using such a configuration[27]. Bahramipanah *et al.* showed the usage of such hybrid structures for enhanced LSPR biosensors[2]. Most of the reports on critical coupling mainly focus on the dielectric layer characteristics and plasmonic resonator behavior for achieving the desired response[24,25]. However, the influence of the mirror layer which has a major role in determining the response has not yet been studied in detail[27–29]. In the current study, we study the effect of mirror characteristics on the critical coupling behavior of plasmonic structures. The response due to metallic mirrors (Ag and Au) as well as dielectric mirrors (dielectric Bragg reflectors) has been studied in detail.

*Corresponding author: (E-mail: shourya@msme.iith.ac.in)

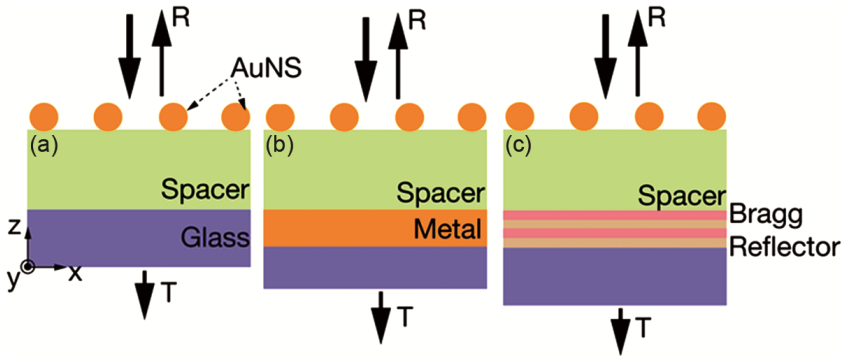

Fig. 1 — Schematic of (a) conventional plasmonic structure, (b) plasmonic structure integrated with a metallic mirror and (c) plasmonic structure with a dielectric Bragg reflector. The spacer is made up of ITO (refractive index of 1.8).

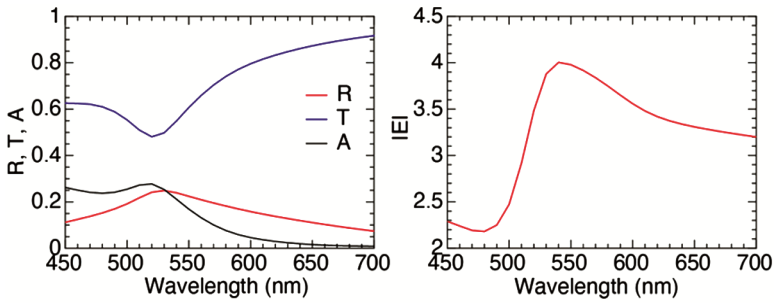

Fig. 2 (a) — Reflection (red), transmission (blue) and absorption (black) spectrum of the bare plasmonic structure. (b) Electric field enhancement as a function of wavelength at a point on the AuNS surface along the polarization direction.

2 Methods

We have used the finite element method software COMSOL Multiphysics (electromagnetic wave module) for calculating the optical response of the plasmonic structures with different substrates. Briefly, a gold nanosphere (AuNS) of 40 nm was placed on top of a dielectric spacer of ITO (refractive index of 1.8).Three different cases were considered: (1) AuNS-ITO placed on top a glass substrate (Fig. 1(a)) & (2) AuNS-ITO placed on top of a metal substrate (Ag or Au) of 40 nm thickness on top of a glass substrate (Fig. 1(b)) & (3) AuNS-ITO placed on top a dielectric Bragg reflector (DBR) on top of a glass substrate (Fig. 1(c)). In each of the simulations, the structure was periodic in the *x*-*y* direction with a periodicity of 50 nm. Periodic boundary conditions were used in the *x*- and *y*-directions. Port boundary was used for truncating the domains in the *z*-direction to obtain a non-reflecting condition on both the top air layer above AuNS (port used for excitation of the plane wave) and bottom glass layer (port used for calculating the scattering parameters).The structure was illuminated from the air with a plane wave propagating in the -*z*-direction and polarized along the *x*-axis. The permittivity of gold was taken from Johnson and Christy data[30]. The refractive index of the substrate was fixed at 1.5.[31]. The AuNS was immersed in air medium (refractive index of 1).The structure was meshed with maximum element size of 10 nm and minimum element size of 0.96 nm. The reflection (R) and transmission (T) from the structure was calculated using the amplitudes of the scattering matrix. The absorption (A) was calculated using the equation: A=1-R-T. To understand the electric field near the AuNS, the near-field enhancement (|E|) was computed at a point on the particle's surface in the direction of polarization (*x*-axis).

3 Results and discussion

Figure 1 shows the three different geometries considered in this study. We first consider the structure with an AuNS placed on top an ITO-glass substrate, which is similar to the conventionally used substrates. The thickness of ITO layer is fixed at 200 nm. Fig. 2(a) shows the optical spectra of the bare plasmonic structure. The resonance wavelength is close to 520 nm as evident from the peak and the dip in the reflection and transmission spectrum, respectively. At resonance, nearly 50% of the intensity is transmitted whereas around 22% is reflected. Consequently, only 28% of the incident light is absorbed by the structure.

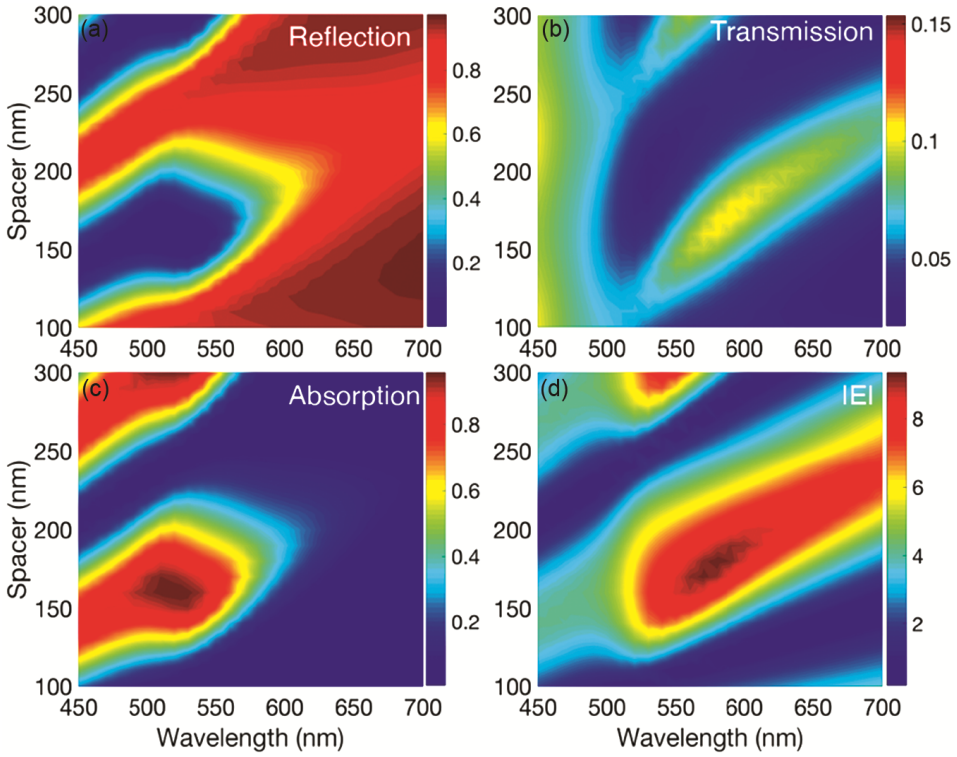

Fig. 3 (a) — Reflection, (b) Transmission, (c) Absorption and (d) Electric field enhancement as a function of wavelength and spacer thickness for the plasmonic structure placed on top of an Ag mirror of 40 nm thickness.

Fig. 2(b) shows the electric field enhancement at a point on the surface of the AuNS along the direction of incident plane wave polarization. Note that this direction corresponds to the highest field enhancement. We observe that the near-field enhancement is around 4 close to 540 nm. Furthermore, the enhancement decreases significantly as one deviates away from the resonance wavelength. The difference in the peak wavelengths from reflection, transmission, and near-field is due to the dispersive nature of the permittivity of gold[32]. It is possible to improve the net absorption and, thereby, the electric field enhancement by using a substrate exhibiting a cavity resonance. Fig. 1(b) and (c) depict the two different types of structures simulated in this study. In Fig. 1(b) the AuNS is placed on top of an ITO layer which is in turn placed on a metallic mirror (either Ag or Au) of 40 nm thickness. In the other case, we have incorporated a DBR reflector instead of a metallic mirror as shown in Fig. 1(c). In both of these cases, the ITO spacer thickness is used as a handle to control the response of the complete structure.

Figure 3(a)-(c) shows the color maps of reflection, transmission and absorption as a function of wavelength and spacer thickness for the case of an Ag mirror (thickness of 40 nm). The reflection color map exhibits minima close to a spacer thickness of 160 nm and wavelength of 520 nm. Correspondingly, the transmission spectrum exhibits a peak as shown in Fig. 3(b). In this structure, the absorption (as calculated from 1-R-T) shows a maximum value for a spacer thickness of 160 nm and wavelength of 520 nm. For this condition, the absorption is nearly 95%. As compared to the bare structure (on ITO-glass), the absorption is enhanced by more than 3 times. This suppression of the reflection and consequently, the enhancement in the absorption is due to the destructive interference of waves reflected from various interfaces. Fig. 3(d) shows the variation of the electric field enhancement as a function of wavelength and spacer thickness. Similar to the optical spectra, we observe a maxima (with a value of 9) in the electric field enhancement for a spacer thickness of 160 nm and wavelength of 570 nm. In this structure, the electric field is enhanced by 2 times as compared to the bare structure.

Figure 4(a)-(c) shows the color maps of reflection, transmission and absorption as a function of wavelength and spacer thickness for the case of Au mirror (thickness of 40 nm). The reflection color map exhibits minima

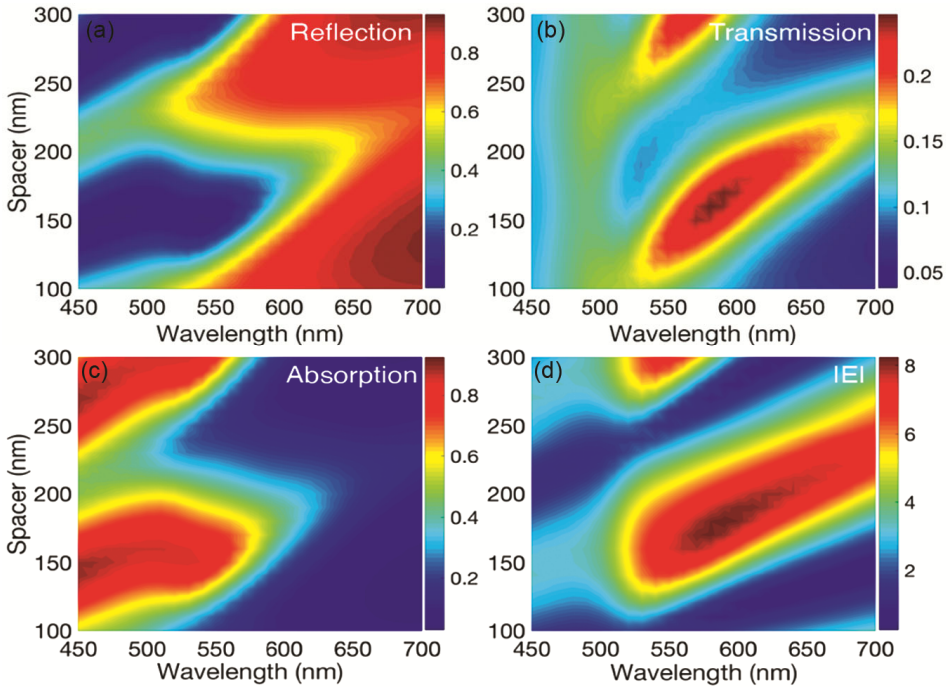

Fig. 4 (a) — Reflection, (b) Transmission, (c) Absorption and (d) Electric field enhancement as a function of wavelength and spacer thickness for the plasmonic structure placed on top of an Au mirror of 40 nm thickness.

close to a spacer thickness of 150 nm and wavelength of 550 nm. For the same parameters, the transmission spectrum exhibits a peak as shown in Fig. 4(b). The absorption in the structure shows a maximum value for a spacer thickness of 160 nm and wavelength of 530 nm. For this condition, the absorption is nearly 84%. As compared to the bare structure, the absorption is enhanced by more than 3 times. But the enhancement for the Au mirror is lower as compared to the Ag mirror case. Fig. 4(d) shows the variation of the electric field enhancement as a function of wavelength and spacer thickness. Similar to the optical spectra, we observe maxima (with a value of 8) in the electric field enhancement for a spacer thickness of 160 nm and wavelength of 560 nm. Even in this structure, the electric field is enhanced by 2 times as compared to the bare structure. Overall, the improvement in the absorption and near-field enhancement is more when an Ag mirror is used as opposed to an Au mirror of identical thickness. This is due to the higher reflectivity and lower losses in Ag as compared to Au. It should be noted that the absorption is also enhanced for wavelengths lower than 500 nm due to the higher losses in gold [30].

Figure 5(a)-(c) shows the color maps of reflection, transmission and absorption as a function of wavelength and spacer thickness for the structure built using a DBR on top of a glass substrate. The DBR was simulated by considering alternate layers of TiO_2 (refractive index of 3.145) and SiO_2 (refractive index of 1.5). The thickness of each layer of TiO_2 and SiO_2wasfixed at 55 nm. In all the simulations, Six repetitions of the layers were considered to realize a DBR with a stop band centered around 550 nm. The reflection color map exhibits minima close to a spacer thickness of 210 nm and wavelength of 520 nm. For the same parameters, the transmission is nearly zero, as shown in Fig. 5(b). The absorption in the structure shows a maximum value for a spacer thickness of 210 nm and wavelength of 520 nm. For this condition, the absorption is nearly 99%. As compared to the bare structure, the absorption is enhanced by more than 3 times. For the structure with DBR, the spectral width of the stop band can be tuned by controlling the thickness of each of the layers. In this case, the stop band is only from around 420 nm to 680 nm. The transmission intensity is high for wavelengths both above and below this range, providing a transparency window that can be used for various applications. As compared to the case of metallic mirrors, the DBR structure leads to higher absorption. Note that the number of layers in the DBR structure is another parameter that can be used for controlling the stop-band characteristics (for example the modulation of the

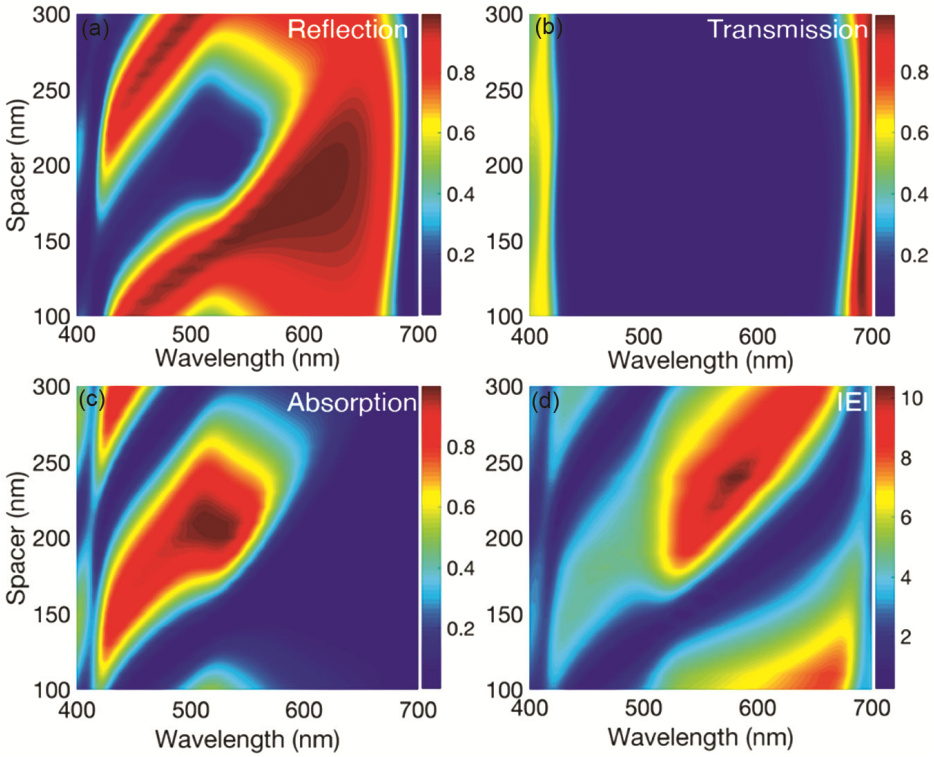

Fig. 5 (a) — Reflection, (b) Transmission, (c) Absorption and (d) Electric field enhancement as a function of wavelength and spacer thickness for the plasmonic structure placed on top a dielectric Bragg reflector (DBR).

reflection in the stop-band) as shown by Lee *et al.*[33]. The variation of the electric field enhancement as a function of wavelength and spacer thickness is shown in Fig. 5(d). Like the optical spectra, we observe a maximum (with a value of 10) in the electric field enhancement for a spacer thickness of 240 nm and wavelength of 575 nm. The electric field is enhanced by 2 times as compared to the bare structure.

From the above results, it is evident that the mirror properties and the spacer thickness determine the optical characteristics of the complete structure. For a specific combination of spacer thickness and wavelengths, the destructive interference of the reflected light from various interfaces leads to the enhancement in the absorption by the structure. In all three cases, it is possible to achieve the enhancement in the absorption in the structure as well as the near-field enhancement as compared to the bare structure. From a fabrication standpoint, the structures with metallic mirrors are easier to fabricate due to the lesser number of depositions required for realizing the structure [2]. On the contrary, using DBR in the structures allows us to fabricate structures that exhibit high absorption close to the plasmon resonance and are transparent at non-resonant wavelengths. Such spectral windows enable the usage of these DBR-incorporated substrates for both imaging (in transmission mode) as well as spectroscopic applications. The results shown in this study provide a clear guideline on the choice of materials used for constructing a critically coupled plasmonic structure and can be used for realizing high-efficiency plasmonic devices.

4 Conclusions

In conclusion, we have studied the effect of mirror properties on the optical response of a critically coupled plasmonic structure. We demonstrate that an appropriate choice of spacer thickness and mirror material, allows us to enhance the optical absorption by more than 3 times. In parallel, the electric field enhancement can be improved by more than 2 times using such tailored substrates. Both metallic and dielectric mirrors (using a DBR stack) were studied, and results show it is possible to achieve high absorption in both these systems. From a practical standpoint, the system with metallic mirrors is easier to fabricate whereas the DBR-based structures open up avenues for realization of multi-functional substrates.

Acknowledgements

S.D.G. would like to acknowledge the funding from DST Grant No. DST/NM/NB/2018/118.

References

1 Mayer K M & Hafner J H, *Chem Rev*, 111 (2011) 3828.
2 Bahramipanah M, Dutta-Gupta S, Abasahl B & Martin O J F, *ACS Nano*, 9 (2015) 7621.
3 Nugroho F A A, Darmadi I, Cusinato L, Susarrey-Arce A, Schreuders H, Bannenberg L J, da Silva F A B, Kadkhodazadeh S, Wagner J B, Antosiewicz T J, Hellman A, Zhdanov V P, Dam B & Langhammer C, *Nat Mater*, 18 (2019) 489.
4 Zhu K, Wang Z, Zong S, Liu Y, Yang K, Li N, Wang Z, Li L, Tang H & Cui Y, *ACS Appl Mater Interfaces*, 12 (2020) 29917.
5 Li C, Liu Y, Zhou X & Wang Y, *J Mater Chem B*, 8 (2020) 3582.
6 Vo-Dinh T, Wang H N & Scaffidi J, *J Biophoton*, 3 (2009) 89.
7 Lane L A, Qian X & Nie S, *Am Chem Soc*, (2015) 10489.
8 Willets K A & van Duyne R P, *Ann Rev Phys Chem*, 58 (2007) 267.
9 Li M, Cushing S K & Wu N, *Analyst*, 140 (2015) 386.
10 Chen H, Kou X, Yang Z, Ni W & Wang J, *Langmuir*, 24 (2008) 5233.
11 Lee K & El-Sayed M A, *J Phys Chem B*, 110 (2006) 19220.
12 Jeon T Y, Park S G, Lee S Y, Jeon H C & Yang S M, *ACS Appl Mater Interfaces*, 5 (2013) 243.
13 Cheng H H, Chen S W, Chang Y Y, Chu J Y, Lin D Z, Chen Y P & Li J H, *Opt Express*, 19 (2011) 22125.
14 Grzelczak M, Pérez-Juste J, Mulvaney P & Liz-Marzán L M, *Chem Soc Rev*, 37 (2008) 1783.
15 Lassiter J B, Sobhani H, Fan J A, Kundu J, Capasso F, Nordlander P & Halas N J, *Nano Lett*, 10 (2010) 3184.
16 Nehl C L, Liao H & Hafner J H, *Nano Lett*, 6 (2006) 683.
17 Cao J, Sun T, Grattan K T V, *Sens Actuators B: Chem*, (2014) 332.
18 Butet J, Yang K Y, Dutta G S & Martin O J F, *ACS Photon*, 3 (2016) 1453.
19 Kasani S, Curtin K & Wu N, *Nanophoton*, 8 (2019) 2065.
20 Ng C, Wesemann L, Panchenko E, Song J, Davis T J, Roberts A & Gómez D E, *Adv Opt Mater*, 7 (2019) 1801660.
21 Artar A, Yanik A A & Altug H, *Appl Phys Lett*, 95 (2009) 051105.
22 Dutta G S & Deb S, *J Opt*, 12 (2010) 075103.
23 Deb S, Gupta S D, Banerji J & Gupta S D, *J Opt A: Pure Appl Opt*, 9 (2007) 555.
24 Liu N, Mesch M, Weiss T, Hentschel M & Giessen H, *Nano Lett*, 10 (2010) 2342.
25 Ameling R, Langguth L, Hentschel M, Mesch M, Braun P V & Giessen H, *Appl Phys Lett*, 97 (2010) 2010.
26 Cesario J, Quidant R, Badenes G & Enoch S, *Opt Lett*, 30 (2005) 3404.
27 Tischler J R, Bradley M S & Bulović V, *Opt Lett*, 31 (2006) 2045.
28 Papanikolaou N, *Phys Rev B*, 75 (2007) 235426.
29 Mock J J, Hill R T, Degiron A, Zauscher S, Chilkoti A & Smith D R, *Nano Lett*, 8 (2008) 2245.
30 Johnson P B & Christy R W, *Phys Rev B*, 6 (1972) 4370.
31 Lévêque G & Martin O J F, *Opt Lett*, 31 (2006) 2750.
32 Zuloaga J & Nordlander P, *Nano Lett*, 11 (2011) 1280.
33 Lee S, Heo H & Kim S, *Sci Rep*, 9 (2019) 4294.